

Article

Influence of Thickness on the Structure and Biological Response of Cu-O Coatings Deposited on cpTi

Ivana Ilievska ^{1,*}, Veronika Ivanova ², Dimitar Dechev ¹, Nikolay Ivanov ¹, Maria Ormanova ¹, Maria P. Nikolova ³ , Yordan Handzhiyski ², Andreana Andreeva ⁴, Stefan Valkov ^{1,5,*}  and Margarita D. Apostolova ² 

¹ Institute of Electronics, Bulgarian Academy of Sciences, 72 Tzarigradsko Chaussee Blvd., 1784 Sofia, Bulgaria; dadechev@abv.bg (D.D.); nick_ivanov_sl@abv.bg (N.I.); m.ormanova@ie.bas.bg (M.O.)

² Roumen Tsanev Institute of Molecular Biology, Bulgarian Academy of Sciences, Acad. G. Bonchev Str., Bl. 21, 1113 Sofia, Bulgaria; veri55@abv.bg (V.I.); folie@abv.bg (Y.H.); margo@obzor.bio21.bas.bg (M.D.A.)

³ Department of Material Science and Technology, University of Ruse, 8 Studentska Str., 7017 Ruse, Bulgaria; mpnikolova@uni-ruse.bg

⁴ Faculty of Physics, Sofia University, 5 James Bourchier Blvd., 1164 Sofia, Bulgaria; andreana@phys.uni-sofia.bg

⁵ Department of Mathematics, Informatics and Natural Sciences, Technical University of Gabrovo, 4 H. Dimitar Str., 5300 Gabrovo, Bulgaria

* Correspondence: ivannyilievsk@gmail.com (I.I.); stsvalkov@gmail.com (S.V.)

Abstract: This work presents results on the influence of thickness on the structure and biological response of Cu-O coatings deposited on commercially pure titanium (cpTi) substrates using direct current (DC) magnetron sputtering. The deposition times were 5, 10, and 15 min to obtain coatings with different thicknesses. The results show that the films deposited for 5, 10, and 15 min correspond to thicknesses of 41, 74, and 125 nm, respectively. The phase composition of the coatings is in the form of a double-phase structure of CuO and Cu₂O in all considered cases. The roughness is on the nanometric scale and no obvious trend as a function of the thickness can be observed for the deposited films. Also, it was found that, with an increase in the thickness of the films, the distribution of the heights becomes closer to symmetrical. The antimicrobial efficacy of different Cu-O-coated cpTi substrates was examined using a direct contact experiment. A possible bactericidal effect was investigated by inoculating a 200 µL bacterial suspension on CuO-coated cpTi and cpTi (control) for 24 h at 37 °C. The results showed that Cu-O-coated cpTi substrates have a 50%–60% higher antimicrobial activity than the substrate. At the same time, human osteosarcoma (MG-63) cells growing on Cu-O-coated cpTi substrates showed 80% viability following 24 h incubation. Depending on magnetron sputtering process parameters, a different coating thickness, various crystallite phase compositions, and diverse biocompatibility were obtained.

Keywords: Cu-O coatings; surface roughness; corrosion resistance; biological response; antimicrobial efficiency; magnetron sputtering



Citation: Ilievska, I.; Ivanova, V.; Dechev, D.; Ivanov, N.; Ormanova, M.; Nikolova, M.P.; Handzhiyski, Y.; Andreeva, A.; Valkov, S.; Apostolova, M.D. Influence of Thickness on the Structure and Biological Response of Cu-O Coatings Deposited on cpTi. *Coatings* **2024**, *14*, 455. <https://doi.org/10.3390/coatings14040455>

Academic Editor: Manuel António Peralta Evaristo

Received: 12 March 2024

Revised: 3 April 2024

Accepted: 8 April 2024

Published: 10 April 2024



Copyright: © 2024 by the authors. Licensee MDPI, Basel, Switzerland. This article is an open access article distributed under the terms and conditions of the Creative Commons Attribution (CC BY) license (<https://creativecommons.org/licenses/by/4.0/>).

1. Introduction

Metals and alloys take a central place amongst medicinal materials used in a large variety of biomedical appliances. The fundamentals of metallic bonding give rise to the general characteristics of metals. The formation and manipulation of medical alloys, as well as their composition, give rise to the physical, mechanical, and biological characteristics that dictate their clinical efficacy [1]. Due to its excellent mechanical characteristics, desirable corrosion resistance, and acceptable biocompatibility, titanium (Ti) and its alloys have been utilized extensively for orthopedic implants [2–5]. Nevertheless, titanium and titanium alloys still have inadequate osteogenic qualities and are prone to bacterial infections [6,7]. Aside from the orthopedic sector, over the years Ti alloys and biomaterials have improved in orthodontics as well, allowing dental treatment to approach the ideal of light continuous forces to achieve rapid tooth movement without damaging teeth or periodontal tissues [8,9].

Nevertheless, inflammatory disease around the implants often leads to the loss of surrounding bones. Consequently, it affects the longevity of the implants, which is the most common cause of their failure. Once a bacterial infection occurs, biofilms on the implant surface fabricated by bacterial colonies will protect bacteria against the host immune system, which will require expensive and complicated clinical treatments, even leading to the failure of orthopedic implant surgery and patient mortality. Therefore, preventing bacterial invasion is essential to ensure the realization of implantation, and improving the antimicrobial properties of implant materials is a pressing necessity [10,11].

All the disadvantages mentioned above depend mostly on the surface properties of the alloy and can be overcome by an appropriate technology for surface modification. There exist several methods for the modification of the surface of metals and alloys, including thin film deposition [12,13], surface treatment by high energy fluxes (electron beam [14–16], laser beam [17,18], etc.), and so on. Currently, one of the most promising methods for the modification of the surface properties of the materials is the deposition of thin films and coatings. Many techniques and methods exist for the deposition of thin films, such as chemical vapor deposition (CVD) [19,20], physical vapor deposition (PVD) [21,22], and others. Nowadays, the direct current (DC) magnetron sputtering technology, which belongs to the PVD technologies, exhibits several advantages, such as a high reproducibility rate and good control of the technological conditions of the deposition process, and therefore, of the structure and properties of the film. The DC magnetron sputtering technology is based on the bombardment of a target material by highly energetic ions [23]. The resultant thickness of the formed coatings is strongly proportional to the deposition time as proven by Liang et al. [24]. The authors of [25] have studied the effect of the thickness of TiN films deposited by DC and pulsed magnetron sputtering on their crystallographic structure and surface topography. The results showed that an increase in the thickness of the films is accompanied with a reduction in the crystallographic imperfections, changes in the preferred crystallographic orientation, and decrease in the surface roughness. Consequently, magnetron sputtering technology now significantly impacts many application areas, including low friction coatings, corrosion-resistant coatings, coatings and films for modern biomedicine, etc. [26,27]. The authors of [26,27] showed that 3.7 μm thick TiN/TiO₂ bilayer coatings deposited on Ti6Al4V alloy by DC magnetron sputtering exhibited high bioactivity and improved corrosion resistance. Also, it was demonstrated that cell attachment strongly depends on the spacing and dimensions of the micro-formations on the surface, while cell viability is influenced by the phase composition and submicron features [27]. It is known that the oxide layer formed on the implant surface supports the adhesion with bone tissue. The authors of [28] showed that the deposition of the TiN/TiO₂ bilayer coating on titanium alloy by DC magnetron sputtering significantly improved wear resistance. At the same time, the hardness and Young's modulus were closer to that of the conical bone, which could open novel practical applications for these materials [28]. Similarly, the study performed in [29] investigated the influence of the preliminary electron-beam treatment of the Co-Cr substrate on the surface topography and friction coefficient of the deposited bilayer TiN/TiO₂ coating. The results showed that the preliminary treatment procedure led to an increase in the surface roughness in the nanometric range and improvement of the wear resistance. These features could have significant importance from a practical point of view in modern biomedicine.

Nevertheless, the Ti-based materials have some disadvantages, such as bio-inertness. This feature can be overcome by doping with bioactive metals like copper [30]. Copper (Cu) showed evidence of promising antimicrobial ability [31]. Moreover, the enhanced antibacterial properties of Cu-O based structures could also have some practical applications in the field of modern biomedicine [32,33]. The authors of [32] have studied the bacterial activity of CuO nanoparticles on immobilized silica films against *E. coli* bacteria. The sol-gel technique on a soda lime glass substrate formed the films. The results showed an improvement in the antibacterial properties against the bacteria. The authors of [33] have investigated the biocompatibility, corrosion resistance, and antibacterial activity of TiO₂/CuO coatings

deposited on a Ti substrate using pulsed magnetron sputtering of Ti target with Cu wires inserted inside. The samples were further annealed to form the oxide phases. The results showed a significant improvement in the biological response, corrosion resistance, and antibacterial properties of the coated implant material. Our previous study [34] showed the possibility of successful deposition of CuO coatings on stainless steel substrates by reactive magnetron sputtering. The results demonstrated that all coatings are in the form of a monoclinic structure. The increase in the substrate temperature during the deposition of the coatings was accompanied by a change in the orientation of the crystallites from (022) to (110) and by a decrease in the concentration of imperfections [34].

After a thorough review of the scientific literature, it is evident that CuO-based structures are very promising in the field of modern biomedicine and biomedical science. However, data related to the biological response and corrosion resistance of Cu-O films deposited on Ti substrates by reactive magnetron sputtering in an argon–oxygen atmosphere, with thicknesses ranging from about 40 to 125 nm are currently less well investigated. The data available within the scientific literature exhibit results corresponding to the biological, antibacterial, and corrosion properties of composite films and coatings where the Cu-O structures were immobilized on the surface of silica films [32], the Cu-O phases are mixed with TiO-based ones [33], etc. Moreover, the influence of the thickness of Cu-O coatings deposited on a Ti substrate on the structure, biological performance, and corrosion resistance within the above-mentioned range has not yet been studied. Therefore, the main purpose of this work is to analyze the influence of thickness on the structure, biological response, and corrosion resistance of Cu-O films deposited on commercially pure titanium (cpTi) substrates by reactive magnetron sputtering.

2. Materials and Methods

Copper oxide coatings were deposited on commercially pure titanium (cpTi) foil with dimensions of 13×13 and thickness of 0.1 mm substrates by reactive direct current (DC) magnetron sputtering. Before deposition, the substrates were etched by Ar ions for 10 min to remove surface contaminations. The copper target used for the experiments had a diameter of 100 mm and a purity of 99.9%. The distance between the substrates and the target was 120 mm. The process took place in an Ar-O₂ atmosphere at a working pressure of 5×10^{-2} Pa. During the deposition process, the substrates were heated to 400 °C; the discharge current was 0.5 A; the discharge voltage was 370 V. The deposition time was varied between 5 and 15 min to obtain coatings with different thicknesses. Three deposition times were used in these experiments, namely 5, 10, and 15 min, corresponding to thicknesses of about 40, 74, and 125 nm, respectively. These thicknesses were directly measured during the cross-sectional SEM observation of the deposited coatings. Ten measurements were performed at each sample and estimated thickness values were obtained after averaging.

The influence of the deposition time and thickness on the phase composition of the deposited Cu-O coatings was investigated by X-ray diffraction (XRD). The experiments were performed in Grazing Incidence Asymmetric Bragg Diffraction (GIABD) mode where CuK α characteristic radiation (1.54 Å) was used. The measurements were realized from 30 to 60° with a step of 0.05° and counting time of 1 s per step.

The structure and chemical composition were studied using Scanning electron microscopy (SEM) and energy-dispersive X-ray spectroscopy (EDX). The measurements were performed on a LYRA 3 I XMU (Tescan, Brno, Czech Republic) electron microscope unit equipped with a detector for EDX investigations (Quantax 200, Bruker, Billerica, MA, USA). The measurements were taken using secondary and back-scattered electrons.

The surface topography and architecture of the deposited coatings were studied using atomic force microscopy (AFM). The measurements were conducted in non-contact mode, with a tip radius of 10 nm. A small, scanned area of $5 \mu\text{m} \times 5 \mu\text{m}$ along the x- and y-axes was chosen. The surface roughness was studied in 6 different zones for each considered sample. The average values for S_a and S_{sk} are presented in the results below.

Electrochemical tests were carried out in an SBF solution using potentiostat/galvanostat Interface 1010E (Gamry Instruments, Warminster, PA, USA). The measurements were conducted in a three-electrode cell-working electrode with 1 cm² of exposed area in SBF solution, a platinum wire as an auxiliary electrode, and Ag/AgCl as a reference electrode. The SBF solution was prepared by sequent dissolving of NaCl, NaHCO₃, KCl, K₂HPO₄·3H₂O, MgCl₂·6H₂O, CaCl₂, and Na₂SO₄ in distilled water and buffered at pH 7.4 with tris hydroxymethyl-aminomethane ((CH₂OH)₃CNH₂) and 1N HCl at 37 °C, according to [35]. The ion concentration in the solution was almost equal to that in human blood plasma. Before the potentiodynamic measurements, the samples were immersed in SBF at 37 °C for 3300 s to establish balanced open circuit potential. The potentiodynamic polarization curves were measured with the initial potential of −250 mV and the final potential of 750 mV vs. OPC at a speed of 0.167 mV/s. Tafel extrapolation method was used to estimate the corrosion current density (j_{corr}) and corrosion potential (E_{corr}).

The measurements of the static contact angle employed the sessile drop method. The samples were cleaned with ethanol and heated at 50 °C for 30 min to remove all possible volatile organic residues. Then, three drops (5 µL) of deionized water were consecutively put on the surface of each sample to report reliable average values. A series of images of three drops on each surface were captured at constant time intervals for 300 s at room temperature. At the end of the sequence, advancing contact angles (\pm standard deviation values) were obtained. The contact angle values were measured from photos using AutoCAD 2016 software.

The antibacterial properties of Cu-O coatings deposited on cpTi foil and uncoated cpTi samples were tested using an *Escherichia coli* (K12, AB1157 (F-thr-1 leu-6 proA2 his-4 argE3 thi-1 lacY1 galK2 ara-14 xyl-5 mtl-1 tsx-33 rspL31 supE44)) Gram-negative strain. It was purchased from the National Bank for Industrial Microorganisms and Cell Cultures (Sofia, Bulgaria). A single colony of *E. coli* was grown overnight in a 5 mL Lysogeny broth (LB) medium containing 1% protein hydrolysate, 0.5% yeast extract, and 0.5% NaCl adjusted to pH 7.4. Cells were cultivated overnight at 37 °C. The next day, 100 µL of these cells was taken from 10 mL of new LB medium and cultured at 37 °C to 0.6 OD. Then, 1 mL of cells was centrifuged for 5 min at 2500 rpm. The supernatant was discarded, and the bacterial pellet was dissolved in 1 mL sterile PBS. The tested layers were placed into 12-well culture plates, covered with 100 µL of the cell suspension, and incubated at 37 °C for 24 h. After incubation, aliquots of 10 µL were taken and diluted 100,000 times. A 100 µL sample taken from the dilution was seeded on LB agar plates. After 24 h incubation at 37 °C, the bacterial colonies were pictured and counted. The following formula was used to calculate the inhibition percentage:

$$R\% = (B - A)/B \times 100 \quad (1)$$

A and B are the colony numbers in the test and control samples, respectively.

The influence of the Cu-O coatings deposited on commercially pure titanium (cpTi) substrates on the cell attachment and growth was assessed with human osteoblast-like MG-63 cells (CRL-1427). The cells were maintained in high glucose (4.5 mg/L) DMEM (Dulbecco's Modified Eagle's Medium, Gibco, Life technologies Ltd., Paisley, UK) containing 10% fetal bovine serum (FBS, Lonza, Switzerland), 100 units/mL penicillin, and 100 µg/mL streptomycin in a humidified CO₂ atmosphere at 37 °C. They were routinely checked for mycoplasma contamination by 4',6-Diamidin-2-phenylindol staining (DAPI, Roche Diagnostics, Mannheim, Germany) and were found free of it.

The cell adhesion assay was carried out by plating 6.5×10^4 MG-63 cells on the substrates for 3 h. After that, nonadherent cells were washed off, and 10 µL of 5 mg/mL concentration MTT (3-(4,5-dimethylthiazol-2-yl)-2,5-diphenyltetrazolium bromide) was added to the remaining cells on each substrate and further incubated at 37 °C for 3 h. The formazan was extracted with isopropanol, and the absorbance was read at 550/630 nm with a DTX880 plate reader (Beckman Coulter, Wals, Austria) to calculate the percentage of cell adhesion.

For cell viability assay, the cells were seeded with 1×10^4 cells/100 μL density in complete DMEM media on $13 \times 13 \text{ mm}^2$ samples in sterile plates for 24 h. Cell viability was determined using the MTT assay [36] and the conditions stated above.

All experiments were conducted with two samples in three independent technical reports. Analysis of variance (ANOVA) and Bonferroni's post hoc test were used to assess the data. A difference in the results was deemed statistically significant if it was at least $p < 0.05$. The statistical software tool PASW 18.0 (IBM, Armonk, NY, USA) for Windows was used for statistical analysis.

3. Results and Discussion

As mentioned in the Section 2, the thickness of the layers deposited for 5, 10, and 15 min was estimated to be 41, 74, and 125 nm, respectively. The thickness measurements were taken using SEM observations of the cross-sections of the specimens. A cross-sectional SEM micrograph of the coating deposited for 15 min is shown in Figure 1, where the thickness of the coating was directly measured. The obtained values for all coatings are in agreement with the linear function given by the authors of Ref. [24].

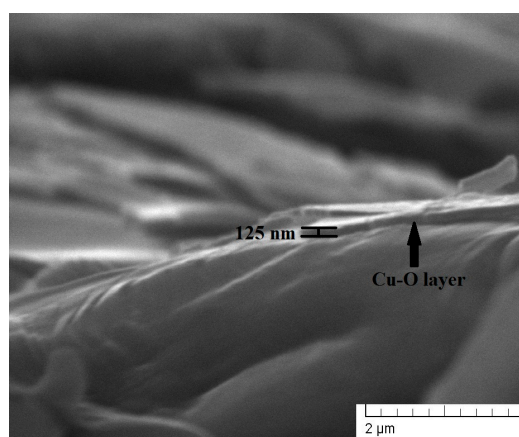


Figure 1. A cross-sectional SEM image of the Cu-O coating deposited for 15 min.

Figure 2a presents the obtained XRD pattern for cpTi used as a standard reference. This diffractogram is typical for substrates consisting purely of the αTi phase characterized with a hexagonal closed packed (hcp) structure. Figure 2b presents the XRD patterns of the coatings deposited at different times of deposition, 5 min, 10 min, and 15 min, respectively. All diffraction maxima are indexed, and all three patterns exhibit a relatively low background. Amorphous-like halos were not observed at the lower Bragg angles, which mean crystal structures were detected without additions of amorphous structures in all considered cases. The diffractograms are typical for polycrystalline materials. In addition to the peaks belonging to the $\alpha\text{-Ti}$ substrate, the patterns exhibit diffraction maxima corresponding to CuO and Cu₂O phases. The phase identification was performed according to the International Center for Diffraction Data (ICDD) Database file Powder Diffraction File (PDF) #05-0661 for the CuO, #05-0667 for the Cu₂O, and #44-1294 for the αTi crystal phase. The obtained coatings are in the form of a double-phase structure of the Cu-O mentioned in the above configurations. It is important to note that the phase composition of the deposited coatings remains the same for all deposition times considered in this study, which means that the thickness of the coatings, ranging from 41 to 125 nm, does not influence the studied structural parameter. The intensity of the peaks corresponding to the phases CuO and Cu₂O becomes higher in cases of deposition for 10 and 15 min. Since the experiments were performed in the GIXRD mode there is no substantial difference in the intensities of the peaks corresponding to the samples deposited at 10 min and 15 min. It is important to note that the peak positions of the coatings deposited for 5, 10, and 15 min are not significantly shifted, meaning that the lattice parameters and volumes are not changed

and, therefore, independent from the deposition time and coating's thickness. This means that the binding forces between the atoms of the deposited coatings for different deposition times of the CuO and Cu₂O phases remain unchanged. This could be of major importance for the corresponding functional properties of the deposited coatings. The results obtained by the authors of [37] showed that the higher values of the lattice constants and the unit cell volume resulted in a lower Young's modulus of Ti-Ta alloys. Similar results were reported by Valkov et al. [38], where the higher unit cell volumes correspond to lower values of the Young's modulus.

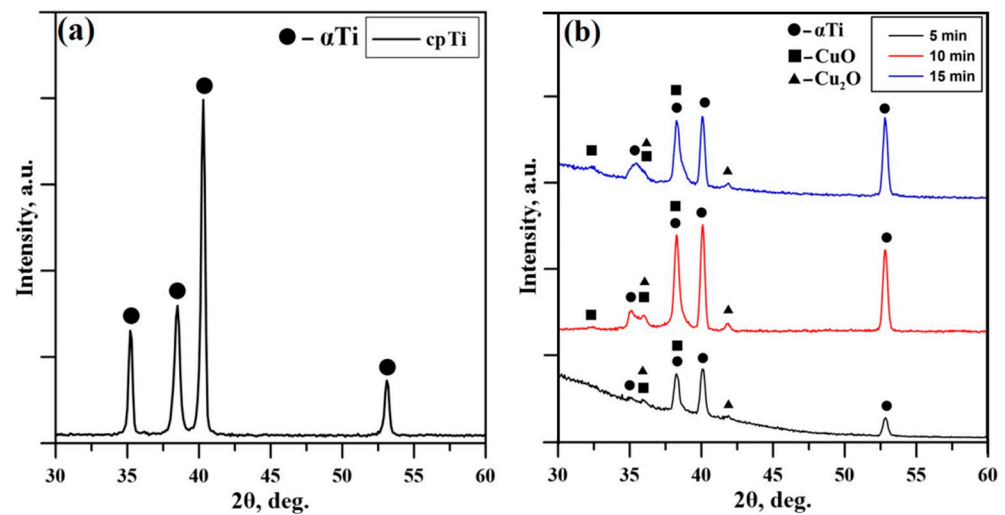


Figure 2. XRD pattern of the (a) cpTi substrate and XRD patterns of the (b) deposited coatings at 5 min, 10 min, and 15 min.

The chemical composition of the samples was studied by energy-dispersive X-ray spectroscopy (EDX) and the results are summarized in Table 1. It is clear that the amount of Cu slightly increases with the rise of the deposition time of the films, which can be attributed to the higher thickness. As already mentioned, the longer deposition time corresponds to films with higher thickness.

Table 1. Chemical composition on the surface of the coatings deposited for 5, 10, and 15 min.

Sample	Ti, at%	Cu, at%	O, at%
5 min	63.94 ± 3.6%	2.67 ± 0.5%	33.39 ± 22.6%
10 min	43.52 ± 2.1%	4.96 ± 0.5%	51.52 ± 44.1%
15 min	27.82 ± 1.5%	7.50 ± 0.6%	64.68 ± 60.7%

Figure 3 displays the AFM images of Cu-O thin films deposited at different times at 5, 10, and 15 min, respectively. The impact of thickness on the topography of the surfaces of the examined samples was quantitatively characterized via the mean roughness value, S_a (Table 1), where higher values of this parameter correspond to rougher surface and vice versa. Further evaluation of the distribution of the measured heights of peaks and depths of valleys was performed by the S_{sk} parameter. The relevance of this parameter to zero is more important than its absolute value. If the heights of peaks are similar to the valleys' depths, the S_{sk} is close to zero. In cases where the value of S_{sk} is far from zero, the distribution of the heights of peaks and depths of valleys is far from symmetric, whereas the positive values of the discussed parameter correspond to higher heights of peaks than depths of valleys and vice versa. The results obtained for the above-discussed parameters are presented in Table 2.

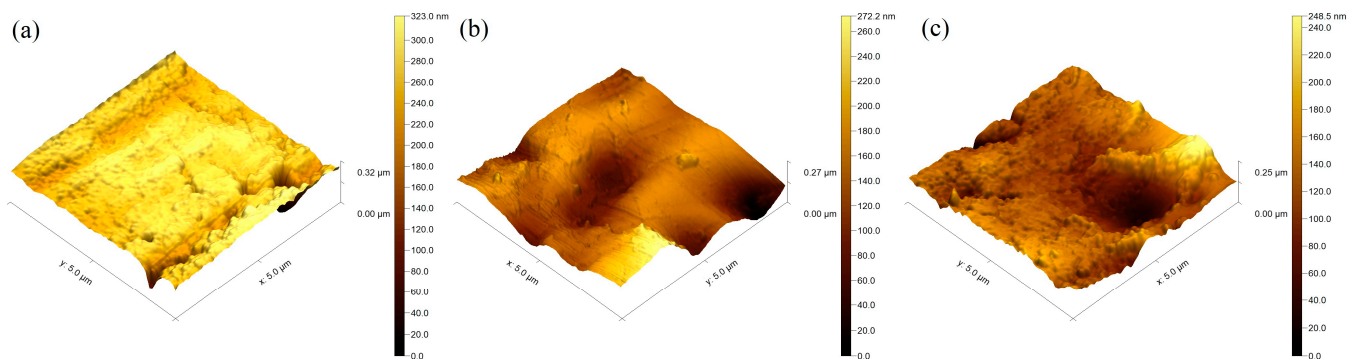


Figure 3. Surface topography of the coatings deposited for (a) 5 min; (b) 10 min; (c) 15 min.

Table 2. The parameters characterizing the thickness, surface topography (S_a), and empiric parameters characterize the asymmetry in the distribution (S_{sk}) of the investigated samples.

Sample	Thickness, nm	S_a , nm	S_{sk}
5 min	41	27.57 ± 7.84	-1.62
10 min	74	52.96 ± 12.15	-0.38
15 min	125	40.40 ± 10.56	-0.33

In light of the results summarized in Table 2, it is evident that the S_{sk} parameter for the coatings deposited for 5, 10, and 15 min has a negative value, meaning that the depths of valleys are higher than the height of peaks. Also, it is important to note that, with an increase in the thickness of the Cu-O films, the S_{sk} parameter becomes closer to zero, meaning that the distribution of the heights becomes closer to symmetrical, which could have some advantages from a practical point of view. These results are in agreement with those published in Ref. [25]. The results obtained for the surface roughness are also presented in Table 2. The surface roughness corresponding to the film deposited for a time of 5 min is 27 nm, and it slightly increases to about 54 nm for a deposition time of 10 min, followed by a slight decrease to 40 nm for a deposition time of 15 min. In all cases, the roughness is on the nanometric scale and again could have some benefits from a practical point of view and for implementation in the field of modern biomedicine. No obvious trend as a function of the thickness can be observed for the deposited films, which is not consistent with the results published in Ref. [25]. However, the thickness deviation in the present particular case is only about 40 nm between the considered films, and in this case, the thickness difference is too small to influence the surface roughness significantly. The results published in Ref. [25] presented the influence of the thickness of TiN coatings on the surface roughness and the results indicated that the latter changes along with the thickness of the coatings. The authors suggest that a major increase in the thickness of the coatings results in a slight decrease in the surface roughness. However, the studied deviation of the thickness of the coatings in Ref. [25] is significantly higher compared to the one investigated in the present study. It is important to note that the surface roughness of the deposited coatings strongly depends on the topography of the Ti substrate. Rougher areas of the base material correspond to coatings with higher values of the S_a parameter and the deposition time does not influence the overall surface roughness, and the topography of the coatings is fully influenced by the topography of the Ti substrate. Higher values for the surface roughness could have some advantages from a practical point of view due to the greater contact area on the surface.

After implantation, the implant surface corrodes in the physiological media, which substantially affects its biocompatibility and long-term life. For that reason, to estimate the corrosion resistance of the coated implant materials, electrochemical measurements were conducted. Figure 4 shows the potentiodynamic polarization curves of the substrate and coated samples while Table 3 lists the values of the corrosion potential (E_{corr}) and corrosion current density (j_{corr}) calculated from the polarization curves using the Tafel

extrapolation method. The results indicate that the corrosion current density of the coated samples is smaller than that of the uncoated specimen, and their corrosion potentials are higher. These results correspond well with a higher value of the contact angle with the SBF solution. Therefore, the copper oxide films demonstrate a role as a stable and protective passive layer. The current density of the pure Ti in the anodic scanning area initially increased and then decreased, indicating that the substrate undergoes anodic dissolution and then produces a passive layer. As noticed earlier, the phase composition of the deposited coatings did not change for all deposition times. The electrochemical results confirmed this observation. The corrosion potential (E_{corr}) and corrosion current density (j_{corr}) values of the oxide-coated films almost overlap because of the formation of similar dense coatings that block the diffusion paths for the corrosive media to pass through defects and reach the substrate [39]. Moreover, Adelojo et al. [40] found that coatings containing a mixture of Cu_2O and CuO demonstrated higher corrosion resistance in chloride- and bicarbonate-containing solutions than specimens with layers of only Cu_2O ; these findings correspond to our results where the mixed Cu_2O and CuO coated samples demonstrate better electrochemical performance than the corrosion-resistant pure Ti substrate. If we also consider the surface roughness parameters of the coated sample, it follows that the rougher surfaces of the 10 and 15 min coated samples slowly decrease the corrosion resistance. This is because the surface roughness enlarges the contact area of the coating with the solution, thus increasing the corrosion processes on the surface [41]. The more hydrophilic surface characteristics of 10 and 15 min coated samples may be due to their higher surface roughness that facilitates rapid absorption. The improved wettability corresponds to the number of the hydroxyl group's hydrogen bond formation with the water molecule.

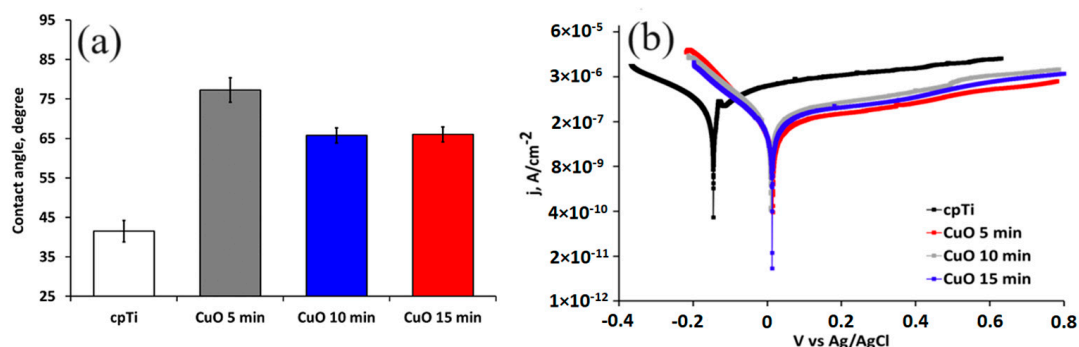


Figure 4. Water contact angle (a) and potentiodynamic polarization curves (b) of the substrate and coated samples in SBF solution at 37 °C.

Table 3. Corrosion potential (E_{corr}), corrosion current density (j_{corr}), and cathodic Tafel region (β_c) values were obtained for the coated samples and substrate.

Sample	E_{corr} (mV)	j_{corr} ($\mu\text{A}/\text{cm}^2$)	β_c (mV/dec)	β_a (mV/dec)
5 min	15.4	0.13	103.8	571
10 min	8.3	0.23	132.9	531
15 min	12.8	0.20	147.5	586
Ti substrate	-145.0	0.29	120.0	65

The Tafel fitting of either the cathodic or anodic polarization curve can determine the corrosion rate. According to He et al. [33], the anodic polarization may be influenced by concentration effects due to dissolution and passivation, which can result in deviation in Tafel behavior while the cathodic curve produces better defined Tafel region. The cathodic Tafel slope β_c (Table 3) of the 15 min coated sample is higher than that of the 5 and 10 min coated one, which verifies the stability and stronger corrosion resistance of the thicker coatings.

Biocompatibility is crucial for medical implants. Therefore, we evaluated MG-63 cell adhesion and viability by culturing the cells on the coated samples. Figure 5a demonstrates MG-63 cell adhesion on the surface of the non-coated (cpTi) and Cu-O-coated samples after 1 h. The samples coated for 10 and 15 min indicated slightly better cell adhesion than the control. Both showed rougher surfaces where osteoblasts can adhere better than on smoother film. Similar observations were reported by Yan et al. [42]. Since the early adhesion is crucially affected by surface protein adsorption, the surface structure and its chemical composition should also be considered. The highest values of the water contact angle were measured for the 5 min deposited coatings that could hinder cell adhesion, although these values of MG-63 adhesion are higher than those of the most hydrophilic uncoated substrate. This fact shows that the nanostructuring and release of Cu from the surface can alter the molecular and cellular events and surface potential, thus improving cell attachment.

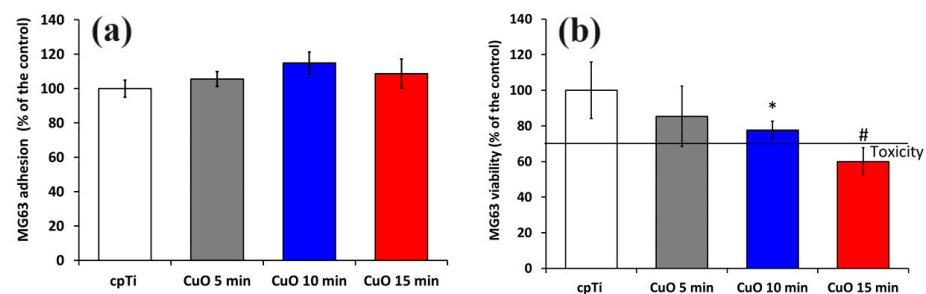


Figure 5. Cell attachment after 3 h (a) and cell viability after 24 h evaluated by MTT assay (b) of MG-63 cells growing on uncoated and coated samples. The results are shown as average \pm SD of three independent technical experiments in duplicates. * $p < 0.05$, # $p < 0.03$ compared to the control sample (cpTi).

An MTT test was used to assess the cytotoxicity of coatings to MG-63 cells. After one day of culturing, the number of cells in the 5 and 10 min coated samples slightly decreased compared to the control. The cpTi substrate and 5 min coated sample exhibited similar cytocompatibility. Taking into account ISO 10993-5 standard, a reduction in cell viability higher than 30% compared to the control can be considered substantially cytotoxic [43]. This indicates that the Cu ion content released from both 5 and 10 min deposited films is within the cell-safe range for the MG-63 cell line.

However, the coatings deposited for 15 min were found to be cytotoxic to MG-63 cells, since the cell viability was reduced down to about 60%, as opposed to the bare Ti; this is possibly due to the higher copper ion concentration in this group. Although copper is an essential trace element, the release of many copper ions may be harmful to cells. As noted earlier [44], the effect of copper on the proliferation of hBMSCs was limited to a small concentration range (50 μ M to 300 μ M). It follows that copper ion release from the 15 min deposited copper oxide coatings for 24 h reduces MG-63 cell viability.

The antibacterial effect of the sputtered copper oxide coatings was determined by a direct contact experiment for 24 h and quantification of viable *E. coli* bacterial cells after that. The obtained results are reported in Figure 6. The viability of bacteria in contact with bare Ti samples was considered the base for calculating the percentage of inhibition of the coated samples. All the tested coatings showed a bactericidal effect. The number of cell colonies after 24 h of incubation with the films reduced substantially (Figure 6a), leading to about 61.0, 73.4, and 79.6% inhibition of the 5, 10, and 15 min deposited coatings as opposed to the bare Ti (Figure 6b), showing very good antibacterial performance. A large number of bacterial colonies were found after incubation with 5 min deposited films demonstrating lower antibacterial activity than those condensed for 10 and 15 min. Consequently, it can be reasonably concluded that the higher deposition time increases the copper content and, therefore, copper ion release from the surface. It was found that the level of copper oxidation, as well as the quantity of copper ions, are crucial for the antimicrobial effect. For

example, Cu^{1+} showed twice lower minimal inhibitory concentration against *E. coli* than that of Cu^{2+} [45]. Also, CuO and Cu_2O exhibit quite different contact-killing behaviors, with Cu_2O having a greater antibacterial effect [46]. Since both CuO and Cu_2O phases are found in all deposited films, the reduction in viable bacteria after incubation with the coatings is possible due to the toxicity of both Cu^{1+} and Cu^{2+} . It is known that copper-containing surfaces can exhibit bactericidal activity through the contact-killing mechanism of copper ions [47] but also that these ions can stimulate the production of reactive oxygen species which participate in the destruction of bacterial cell membranes and cell disintegration [48]. According to Haber–Weiss and Fenton reactions, Ladomersky et al. [49] proposed that an increase in the intrinsic amount of copper leads to significant oxidative stress that is quickly exhibited by redox cycling between the various forms of copper, such as Cu^{1+} and Cu^{2+} . Therefore, regarding the inherent antibacterial properties of Cu-containing coatings, the copper release mechanism may reduce crucial first-day times linked to microbial issues with implants due to contamination during surgery.

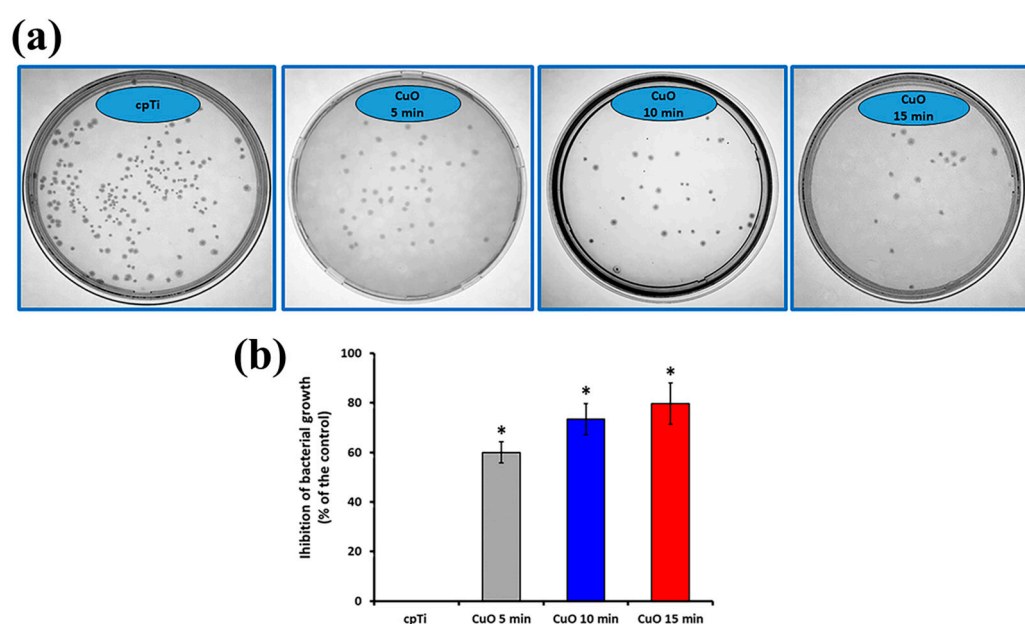


Figure 6. Representative photographs of *E. coli* colonies (a) and the calculated inhibition of bacteria growth (b). The results are shown as average \pm SD of three independent technical experiments in duplicates. * $p < 0.001$ compared to the control sample (cpTi).

The use of thin films promoting osteoblast viability is a promising way to support bone regeneration. Based on the results mentioned above, it follows that an efficient and simple method to impart antimicrobial properties along with acceptable cytotoxicity can be the reactive magnetron sputtering of Cu in an $\text{O}_2 + \text{Ar}$ atmosphere with a controlled time for deposition. However, designing multifunctional Cu-containing sputtered coatings with both improved biocompatibility and antibacterial ability on titanium implants will be the focus of our next research.

4. Conclusions

This study examines results of the biocompatibility of Cu-O-based coatings deposited by DC reactive magnetron sputtering. The coatings were applied to cpTi substrates where the deposition times were 5, 10, and 15 min, corresponding to thicknesses of 41, 74, and 125 nm, respectively. The phase composition of the coatings is in the form of a double-phase structure of CuO and Cu_2O in all considered cases. In all cases, the roughness is on the nanometric scale and no obvious trend as a function of the thickness can be observed for the deposited films. Also, it was found that, with an increase in the thickness of the films, the distribution of the heights becomes closer to symmetrical. The examined films

showed satisfactory biocompatibility. The coated samples were subjected to antimicrobial testing, which verified that copper oxide films exhibited greater antibacterial activity than bare Ti samples. The application of copper oxide coatings resulted in up to 79.6% loss of bacterial viability. The antimicrobial activity increased with increasing the time of deposition. Therefore, notwithstanding some findings, the surface modification reported in this work may still be considered a viable approach for creating antimicrobial coatings on orthopedic implants. Further research is needed to determine its application using different types of bone cells, either in vitro or through in vivo experiments.

Author Contributions: Conceptualization, M.P.N., M.D.A. and S.V.; methodology, M.P.N., M.D.A., S.V., D.D., N.I., I.I., M.O., Y.H., A.A. and V.I.; formal analysis, M.P.N., M.D.A., S.V., D.D., N.I., I.I., M.O., Y.H., A.A. and V.I.; investigation, M.P.N., M.D.A., S.V., D.D., N.I., I.I., M.O., Y.H., A.A. and V.I.; writing—original draft preparation, I.I., M.P.N., M.D.A. and S.V.; writing—review and editing, M.P.N., M.D.A. and S.V.; visualization, M.P.N., M.D.A., M.O. and V.I.; supervision, M.P.N.; project administration, M.P.N. All authors have read and agreed to the published version of the manuscript.

Funding: This research was funded by the Bulgarian National Science Fund, grant number KII-06-H67-5 (2022).

Institutional Review Board Statement: Not applicable.

Informed Consent Statement: Not applicable.

Data Availability Statement: Data are available within the article.

Conflicts of Interest: The authors declare no conflicts of interest.

References

- Minnath, M. Metals and alloys for biomedical applications. In *Fundamental Biomaterials: Metals*; Balakrishnan, P., Sreekala, M., Thimas, S., Eds.; Woodhead Publishing: Sawston, UK, 2018; pp. 167–174.
- Zhang, Y.; Fu, S.; Yang, L.; Qin, G.; Zhang, E. A nano-structured TiO₂/CuO/Cu₂O coating on Ti-Cu alloy with dual function of antibacterial ability and osteogenic activity. *J. Mater. Sci. Technol.* **2022**, *97*, 201–212. [[CrossRef](#)]
- Bordji, K.; Jouzeau, J.Y.; Mainard, D.; Payan, E.; Netter, P.; Rie, K.T.; Stucky, T.; Hage-Ali, M. Cytocompatibility of Ti-6Al-4V and Ti-5Al-2.5Fe alloys according to three surface treatments, using human fibroblasts and osteoblasts. *Biomaterials* **1996**, *17*, 929–940. [[CrossRef](#)] [[PubMed](#)]
- Sittig, C.; Textor, M.; Spencer, N.D.; Wieland, M.; Vallotton, P.H. Surface characterization of implant materials c.p. Ti, Ti-6Al-7Nb and Ti-6Al-4V with different pretreatments. *J. Mater. Sci. Mater. Med.* **1999**, *10*, 35–46. [[CrossRef](#)]
- Zhu, X.; Chen, J.; Scheideler, L.; Reichl, R.; Geis-Gerstorfer, J. Effects of topography and composition of titanium surface oxides on osteoblast responses. *Biomaterials* **2004**, *25*, 4087–4103. [[CrossRef](#)]
- Hsu, H.; Wu, S.; Hsu, S.; Li, C.; Ho, W. Effects of chromium addition on structure and mechanical properties of Ti-5Mo alloy. *Mater. Des.* **2015**, *65*, 700–706. [[CrossRef](#)]
- Zheng, D.; Neoh, K.; Kang, E. Bifunctional coating based on carboxymethyl chitosan with stable conjugated alkaline phosphatase for inhibiting bacterial adhesion and promoting osteogenic differentiation on titanium. *Appl. Surf. Sci.* **2016**, *360*, 86–97. [[CrossRef](#)]
- Marin, E.; Lanzutti, A. Biomedical Applications of Titanium Alloys: A Comprehensive Review. *Materials* **2024**, *17*, 114. [[CrossRef](#)] [[PubMed](#)]
- Ilievska, I. Study of Materials with Orthodontic Application. Ph.D. Thesis, Institute of Solid State Physics, Bulgarian Academy of Sciences, Sofia, Bulgaria, 2018.
- Wu, Y.; Zhou, H.; Zeng, Y.; Xie, H.; Ma, D.; Wang, Z.; Liang, H. Recent Advances in Copper-Doped Titanium Implants. *Materials* **2022**, *15*, 2342. [[CrossRef](#)] [[PubMed](#)]
- van Hoogstraten, S.W.G.; Fechter, J.; Bargon, R.; van Agtmaal, J.L.; Peeters, L.C.W.; Geurts, J.; Arts, J.J.C. The Antibacterial Properties of a Silver Multilayer Coating for the Prevention of Bacterial Biofilm Formation on Orthopedic Implants—An In Vitro Study. *Coatings* **2024**, *14*, 216. [[CrossRef](#)]
- Alontseva, D.; Safarova, Y.; Voinarovych, S.; Obrosova, A.; Yamanoglu, R.; Khoshnaw, F.; Yavuz, H.I.; Nessipbekova, A.; Syzdykova, A.; Azamatov, B.; et al. Biocompatibility and Corrosion of Microplasma-Sprayed Titanium and Tantalum Coatings versus Titanium Alloy. *Coatings* **2024**, *14*, 206. [[CrossRef](#)]
- Ratova, M.; Kelly, P.; West, G.; Iordanova, I. Enhanced properties of magnetron sputtered photocatalytic coatings via transition metal doping. *Surf. Coat. Technol.* **2013**, *228*, S544–S549. [[CrossRef](#)]
- Ivanov, Y.; Gromov, V.; Zagulyaev, D.; Konovalov, S.; Rubannikova, Y. Improvement of Functional Properties of Alloys by Electron Beam Treatment. *Steel Transl.* **2022**, *52*, 71–75. [[CrossRef](#)]
- Zhang, L.; Peng, C.; Guan, J.; Lv, P.; Guan, Q. Nanocrystalline Cr-Ni Alloying Layer Induced by High-Current Pulsed Electron Beam. *Nanomaterials* **2019**, *9*, 74. [[CrossRef](#)] [[PubMed](#)]

16. Zagulyaev, D.; Konovalov, S.; Gromov, V.; Glezer, A.; Ivanov, Y.; Sundeev, R. Structure and properties changes of Al-Si alloy treated by pulsed electron beam. *Mater. Lett.* **2018**, *229*, 377–380. [[CrossRef](#)]
17. Pi, H.; Zhi, G.; Chen, C.; Li, C.; Zhou, J.; Long, Y. Microstructure, Hardness and Corrosion Resistance of Al-TiC MMC Prepared by Laser Cladding on AZ31B Magnesium Alloy. *Coatings* **2024**, *14*, 211. [[CrossRef](#)]
18. Almeida, A.; Petrov, P.; Nogueira, I.; Vilar, R. Structure and properties of Al-Nb alloys produced by laser surface alloying. *Mater. Sci. Eng. A* **2001**, *303*, 273–280. [[CrossRef](#)]
19. Buchkov, K.; Rafailov, P.; Minev, N.; Videva, V.; Strijkova, V.; Lukanov, T.; Dimitrov, D.; Marinova, V. Metatungstate Chemical Vapor Deposition of WSe₂: Substrate Effects, Shapes, and Morphologies. *Crystals* **2024**, *14*, 184. [[CrossRef](#)]
20. Mallik, A.K.; Shih, W.-C.; Pobedinskas, P.; Haenen, K. Early Periods of Low-Temperature Linear Antenna CVD Nucleation and Growth Study of Nanocrystalline Diamond Films. *Coatings* **2024**, *14*, 184. [[CrossRef](#)]
21. Kelly, P.; Barker, P.; Ostovarpour, S.; Ratova, M.; West, G.; Iordanova, I.; Bradley, W. Deposition of photocatalytic titania coatings on polymeric substrates by HiPIMS. *Vacuum* **2012**, *86*, 1880–1882. [[CrossRef](#)]
22. Freeman, J.; Kelly, P.; West, G.; Bradley, W.; Iordanova, I. The effects of composition and pulsed biasing on chromium nitride films. *Surf. Coat. Technol.* **2009**, *204*, 907–910. [[CrossRef](#)]
23. Kelly, P.; Arnell, D. Magnetron sputtering: A review of recent developments and applications. *Vacuum* **2000**, *56*, 159–172. [[CrossRef](#)]
24. Liang, H.; Xu, J.; Zhou, D.; Sun, X.; Chu, S.; Bai, Y. Thickness dependent microstructural and electrical properties of TiN thin films prepared by DC reactive magnetron sputtering. *Ceram. Int.* **2016**, *42*, 2642–2647. [[CrossRef](#)]
25. Iordanova, I.; Kelly, P.; Burova, M.; Andreeva, A.; Stefanova, B. Influence of thickness on the crystallography and surface topography of TiN nano-films deposited by reactive DC and pulsed magnetron sputtering. *Thin Solid Films* **2012**, *520*, 5333–5339. [[CrossRef](#)]
26. Nikolova, M.P.; Nikolova, V.; Ivanova, V.L.; Valkov, S.; Petrov, P.; Apostolova, M.D. Mechanical properties and in vitro biocompatibility evaluation of TiN/TiO₂ coated Ti6Al4V alloy. *Mater. Today Proc.* **2020**, *33*, 1781–1786. [[CrossRef](#)]
27. Nikolova, M.; Ormanova, M.; Nikolova, V.; Apostolova, M.D. Electrochemical, Tribological and Biocompatible Performance of Electron Beam Modified and Coated Ti6Al4V Alloy. *Int. J. Mol. Sci.* **2021**, *22*, 6369. [[CrossRef](#)] [[PubMed](#)]
28. Petrov, P.; Dechev, D.; Ivanov, N.; Hikov, T.; Valkov, S.; Nikolova, M.; Yankov, E.; Parshorov, S.; Bezdushnyi, R.; Andreeva, A. Study of the influence of electron beam treatment of Ti5Al4V substrate on the mechanical properties and surface topography of multilayer TiN/TiO₂ coatings. *Vacuum* **2018**, *154*, 264–271. [[CrossRef](#)]
29. Valkov, S.; Parshorov, S.; Andreeva, A.; Bezdushnyi, R.; Nikolova, M.; Dechev, D.; Ivanov, N.; Petrov, P. Influence of Electron Beam Treatment of Co-Cr Alloy on the Growing Mechanism, Surface Topography, and Mechanical Properties of Deposited TiN/TiO₂ Coatings. *Coatings* **2019**, *9*, 513. [[CrossRef](#)]
30. Wu, C.; Zhou, Y.; Xu, M.; Han, P.; Chen, L.; Chang, J. Copper-containing mesoporous bioactive glass scaffolds with multifunctional properties of angiogenesis capacity, osteostimulation and antibacterial activity. *Biomaterials* **2013**, *34*, 422–433. [[CrossRef](#)] [[PubMed](#)]
31. Kelly, P.; Li, H.; Benson, P.; Whitehead, K.; Verran, J.; Arnell, R.; Iordanova, I. Comparison of the tribological and antimicrobial properties of CrN/Ag, ZrN/Ag, TiN/Ag, and TiN/Cu nanocomposite coatings. *Surf. Coat. Technol.* **2010**, *205*, 1606–1610. [[CrossRef](#)]
32. Akhavan, O.; Ghaderi, E. Cu and CuO nanoparticles immobilized by silica thin films as antibacterial materials and photocatalysts. *Surf. Coat. Technol.* **2010**, *205*, 219–223. [[CrossRef](#)]
33. He, X.; Zhang, G.; Wang, X.; Hang, R.; Huang, X.; Qin, L.; Tang, B.; Zhang, X. Biocompatibility, corrosion resistance and antibacterial activity of TiO₂/CuO coating on titanium. *Ceram. International* **2017**, *43*, 16185–16195. [[CrossRef](#)]
34. Ormanova, M.; Kotlarski, G.; Valkov, S.; Dechev, D.; Ivanov, N.; Petrov, P. Formation and characterization of CuO coatings deposited by reactive magnetron sputtering. *J. Phys. Conf. Ser.* **2021**, *2240*, 012010. [[CrossRef](#)]
35. Kokubo, T.; Kushitani, H.; Sakka, S.; Kitsugi, T.; Yamamuro, T. Solutions able to reproduce in vivo surface-structure changes in bioactive glass-ceramic A-W³. *J. Biomed. Mater. Res.* **1990**, *24*, 721–734. [[CrossRef](#)] [[PubMed](#)]
36. Mosmann, T. Rapid colorimetric assay for cellular growth and survival: Application to proliferation and cytotoxicity assays. *J. Immunol. Methods* **1983**, *65*, 55–63. [[CrossRef](#)] [[PubMed](#)]
37. Zhou, Y.; Niinomi, M.; Akahori, T. Effects of Ta content on Young's modulus and tensile properties of binary Ti-Ta alloys for biomedical applications. *Mater. Sci. Eng. A* **2004**, *371*, 283–290. [[CrossRef](#)]
38. Valkov, S.; Dechev, D.; Ivanov, N.; Bezdushnyi, R.; Ormanova, M.; Petrov, P. Influence of Beam Power on Young's Modulus and Friction Coefficient of Ti-Ta Alloys Formed by Electron-Beam Surface Alloying. *Metals* **2021**, *11*, 1246. [[CrossRef](#)]
39. Ait-Djafer, A.; Saoula, N.; Aknouche, H.; Guedouar, B.; Madaoui, N. Deposition and characterization of titanium aluminum nitride coatings prepared by RF magnetron sputtering. *Appl. Surf. Sci.* **2015**, *350*, 6–9. [[CrossRef](#)]
40. Adeleju, B.; Duan, Y. Corrosion resistance of Cu₂O and CuO on copper surfaces in aqueous media. *Br. Corros. J.* **1994**, *29*, 309–314. [[CrossRef](#)]
41. Zhang, X.; Liu, Z.; Shen, W.; Gurunathan, S. Silver nanoparticles: Synthesis, characterization, properties, applications, and therapeutic approaches. *Int. J. Mol. Sci.* **2016**, *17*, 1534. [[CrossRef](#)] [[PubMed](#)]
42. Yan, Y.; Chibowski, E.; Szcześ, A. Surface properties of Ti-6Al-4V alloy part I: Surface roughness and apparent surface free energy. *Mater. Sci. Eng. C* **2017**, *70*, 207–215. [[CrossRef](#)]

43. ISO 10993-5:2009; Biological Evaluation of Medical Devices Part 5: Tests for Invitro Cytotoxicity. International Organization for Standardization/ANSI: Geneva, Switzerland, 2009.
44. Burghardt, I.; Lüthen, F.; Prinz, C.; Kreikemeyer, B.; Zietz, C.; Neumann, H.; Rychly, J. A dual function of copper in designing regenerative implants. *Biomaterials* **2015**, *44*, 36–44. [[CrossRef](#)] [[PubMed](#)]
45. Saphier, M.; Silberstein, E.; Shotland, Y.; Popov, S.; Saphier, O. Prevalence of monovalent copper over divalent in killing *Escherichia coli* and *Staphylococcus aureus*. *Curr. Microbiol.* **2018**, *75*, 426–430. [[CrossRef](#)] [[PubMed](#)]
46. Hans, M.; Erbe, A.; Mathews, S.; Chen, Y.; Solioz, M.; Mücklich, F. Role of copper oxides in contact killing of bacteria. *Langmuir* **2013**, *29*, 16160–16166. [[CrossRef](#)] [[PubMed](#)]
47. Molteni, C.; Abicht, H.; Solioz, M. Killing of Bacteria by Copper Surfaces Involves Dissolved Copper. *Appl. Environ. Microbiol.* **2010**, *76*, 4099–4101. [[CrossRef](#)] [[PubMed](#)]
48. Ren, Q.; Qin, L.; Jing, F.; Cheng, D.; Wang, Y.; Yang, M.; Xie, D.; Leng, Y.; Akhavan, B.; Huang, N. Reactive magnetron co-sputtering of Ti-xCuO coatings: Multifunctional interfaces for blood-contacting devices. *Mater. Sci. Eng. C* **2020**, *116*, 111198. [[CrossRef](#)]
49. Ladomersky, E.; Petris, M. Copper tolerance and virulence in bacteria. *Metallomics* **2015**, *7*, 957–964. [[CrossRef](#)]

Disclaimer/Publisher’s Note: The statements, opinions and data contained in all publications are solely those of the individual author(s) and contributor(s) and not of MDPI and/or the editor(s). MDPI and/or the editor(s) disclaim responsibility for any injury to people or property resulting from any ideas, methods, instructions or products referred to in the content.